Geophysical Journal International

Geophys. J. Int. (2017) **208,** 118–133
Advance Access publication 2016 October 13
GJI Geodynamics and tectonics

doi: 10.1093/gji/ggw386

Reconciling geodetic and geological estimates of recent plate motion across the Southwest Indian Ridge

C. DeMets,[1] E. Calais[2] and S. Merkouriev[3,4]

[1]*Department of Geoscience, University of Wisconsin-Madison, Madison, WI* 53706*, USA. E-mail: chuck@geology.wisc.edu*
[2]*Department of Geosciences, UMR CNRS* 8538 *Ecole Normale Superieure,* 24 *run Lhomond, F-*75231 *Paris cedex* 05*, France*
[3]*Pushkov Institute of Terrestrial Magnetism of the Russian Academy of Sciences, St Petersburg Filial.* 1 *Mendeleevskaya Liniya, St Petersburg* 199034*, Russia*
[4]*Institute of Earth Sciences, Saint Petersburg State University, Universitetskaya nab.* 7-9*, St. Petersburg* 199034*, Russia*

Accepted 2016 October 9. Received 2016 October 4; in original form 2016 May 26

SUMMARY

We use recently published, high-resolution reconstructions of the Southwest Indian Ridge to test whether a previously described systematic difference between Global Positioning System (GPS) and 3.16-Myr-average estimates of seafloor spreading rates between Antarctica and Africa is evidence for a recent slowdown in Southwest Indian Ridge seafloor spreading rates. Along the Nubia-Antarctic segment of the ridge, seafloor opening rates that are estimated with the new, high-resolution reconstructions and corrected for outward displacement agree well with geodetic rate estimates and reduce previously reported, highly significant non-closure of the Nubia-Antarctic-Sur plate circuit. The observations are inconsistent with a slowdown in spreading rates and instead indicate that Nubia-Antarctic plate motion has been steady since at least 5.2 Ma. Lwandle-Antarctic seafloor spreading rates that are estimated from the new high-resolution reconstructions differ insignificantly from a GPS estimate, thereby implying steady Lwandle-Antarctic plate motion since 5.2 Ma. Between the Somalia and Antarctic plates, the new Southwest Indian Ridge reconstructions eliminate roughly half of the systematic difference between the GPS and MORVEL spreading rate estimates.We interpret the available observations as evidence that Somalia-Antarctic spreading rates have been steady since at least 5.2 Ma and postulate that the remaining difference is attributable to random and/or systematic errors in the plate kinematic estimates and the combined effects of insufficient geodetic sampling of undeforming areas of the Somalia plate, glacial isostatic adjustment in Antarctica and transient deformation triggered by the 1998 $M_w = 8.2$ Antarctic earthquake, the 2004 $M_w = 9.3$ Sumatra earthquake, or possibly other large historic earthquakes.

Key words: Plate motions; Mid-ocean ridge processes; Africa; Antarctica.

1 INTRODUCTION

As one of three long spreading centres that surround Antarctica (Fig. 1), the slow-spreading Southwest Indian Ridge (Southwest Indian Ridge) occupies an important position in the global plate circuit, such that reconstructions of all of the major and many smaller plates in the Indian, Atlantic and Pacific Ocean basins depend to some degree on reconstructions of Southwest Indian Ridge seafloor spreading. For example, plate kinematic estimates of Nubia-Somalia motion across the East African Rift are determined from estimates of Nubia-Antarctic and Somalia-Antarctic plate motions (e.g. Royer *et al.* 2006; Horner-Johnson *et al.* 2007), as are estimates of India-Eurasia (Molnar & Stock 2009) and Pacific-North America plate motions (e.g. Wilson *et al.* 2005). Any errors in the rotations that describe motion across the Southwest Indian Ridge thus have broad potential impacts on global-scale tectonic studies as well as geodynamic studies that use plate rotations to tune or validate their model assumptions and predictions.

This study is motivated by evidence reported by Saria *et al.* (2014) that seafloor spreading rates everywhere along the Southwest Indian Ridge as inferred from the velocities of Global Positioning System (GPS) sites in Africa and Antarctica are 1–2 mm yr^{-1} slower than rates estimated with the MORVEL angular velocities (Fig. 2), which describe plate motions averaged over the past 3.16 Myr (DeMets *et al.* 2010). The difference, which is observed for all three plate pairs that are separated by the ridge (Fig. 2), may be evidence for spreading rate slowdowns for all three plate pairs since 3.16 Myr. Alternatively, the geodetic and/or geological estimates may be biased, the latter possibly due to imprecise calibrations for the influence of outward displacement on magnetic reversal locations (DeMets & Wilson 2008).

Herein, we test between these possibilities using newly available rotations that reconstruct the Southwest Indian Ridge at ∼1 Myr intervals for the past 20 Myr (DeMets *et al.* 2015—hereafter abbreviated DMS15). We evaluate the consistency of the new DMS15 rotation estimates and their associated corrections for biases due

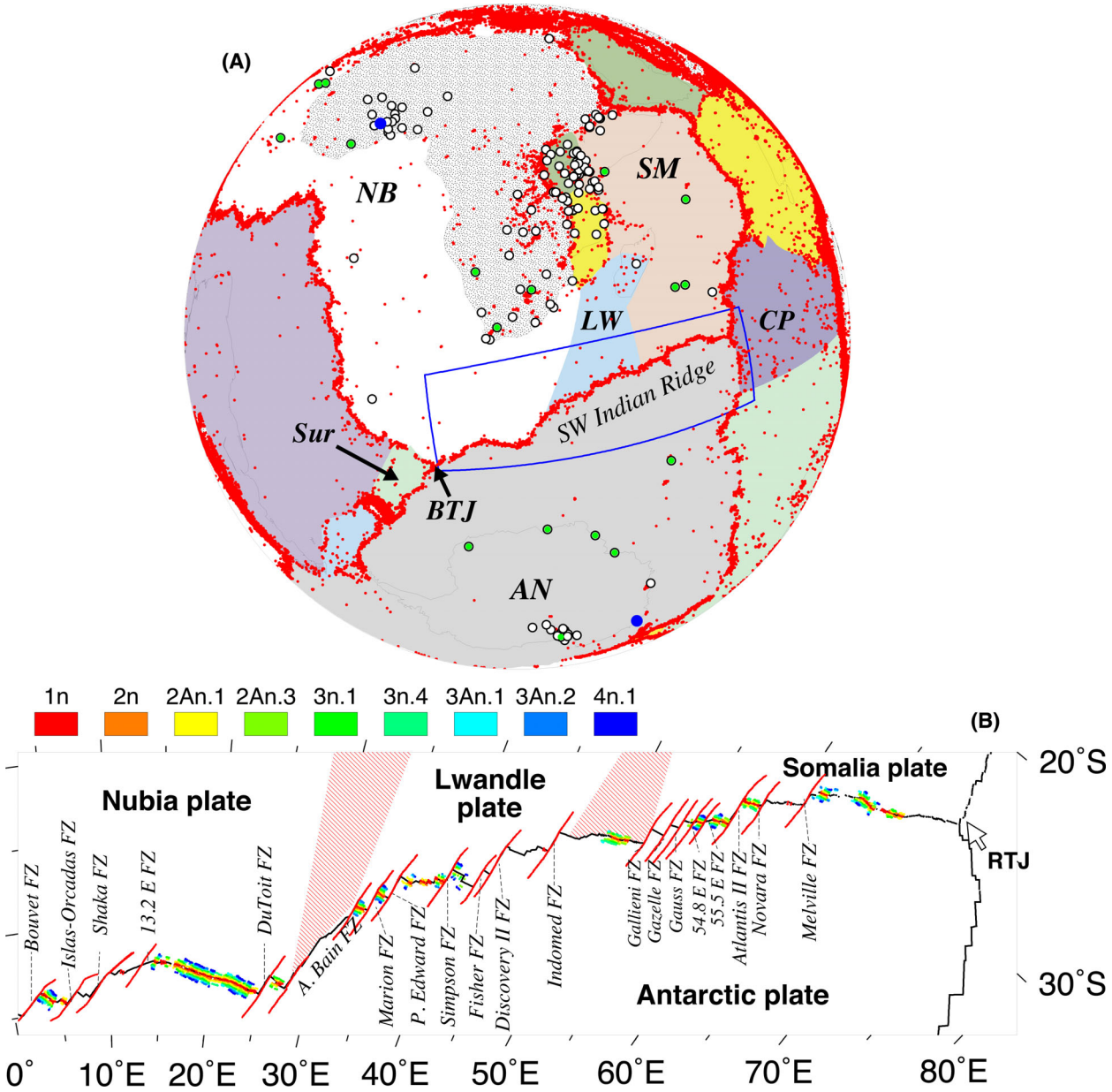

Figure 1. Location maps for the study area. (A) Plate tectonic setting, GPS site locations and 1964–2013 $M > 3.5$ earthquakes above 60 km from www.neic.cr.usgs.gov (red circles). The open and green-filled circles show the locations of GPS sites used by Saria *et al.* (2014) to estimate Antarctic, Nubia, Somalia, Lwandle, Rovuma and Victoria plate angular velocities. The green and blue circles show the locations of GPS sites used by Kreemer *et al.* (2014) to estimate Nubia-Somalia-Antarctic angular velocities. The blue rectangle delimits the region shown in the lower map. (B) Oblique Mercator projection of the Southwest Indian Ridge with prominent transforms labeled. Coloured circles show crossings of magnetic reversals 1n (0.78 Ma) through 4n.1 (7.53 Ma) from DeMets *et al.* (2015). Abbreviations: 'AN': Antarctic plate; 'BTJ': Bouvet triple junction; 'CP': Capricorn plate; 'LW': Lwandle plate; 'NB': Nubia plate; SM: Somalia plate. 'Sur' identifies the location of the Sur microplate (DeMets *et al.* 2010).

to magnetic reversal outward displacement with two recently published and our own GPS estimates of motion across the ridge and with constraints that are imposed by plate-circuit closures around the Bouvet and Rodrigues triple junctions at either end of the Southwest Indian Ridge. Given that angular velocities that are estimated from GPS site velocities are immune to any biases associated with outward displacement, we use geodetic estimates of Southwest Indian Ridge plate motions to test the calibrations for outward displacement that were used by previous authors to correct their plate reconstructions. We also consider whether possible drift of Earth's geocentre in ITRF2008 (Wu *et al.* 2011), regional post-seismic deformation triggered by the $M_w = 8.2$ 1998 Antarctic earthquake (King & Santamaria-Gomez 2016) or $M_w = 9.3$ 2004 December 26 Sumatra earthquake (Pollitz *et al.* 2006; Chlieh *et al.* 2007), or glacial isostatic rebound in Antarctica (King *et al.* 2016) might affect the geodetic estimates enough to alter our main results and conclusions.

2 DATA AND PLATE ROTATIONS

Our analysis is based on data and results from four studies that sample Southwest Indian Ridge plate motions over different timescales. Over timescales of years to decades, we estimate Southwest Indian

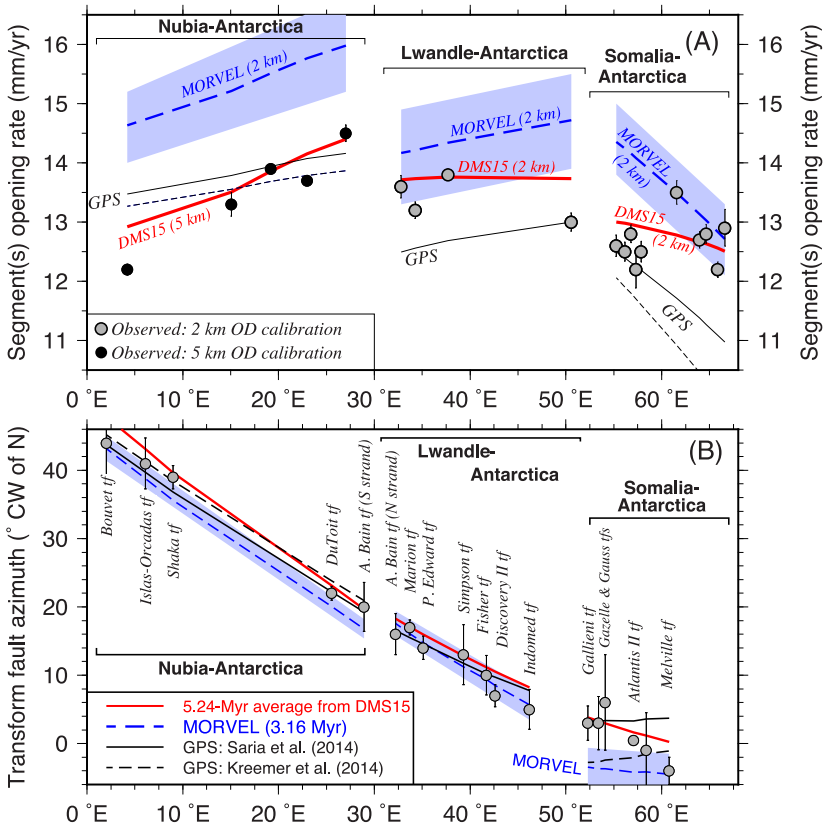

Figure 2. (A) Southwest Indian Ridge spreading rates and (B) transform fault azimuths estimated with the GPS-only angular velocities of Saria *et al.* (2014) and Kreemer *et al.* (2014), the 3.16-Myr-average MORVEL angular velocities (DeMets *et al.* 2010) and 5.24-Myr-average motions estimated with Chron 3n.4 noise-reduced finite rotations from DeMets *et al.* (2015) (see the text). Best estimates of the long-term (5.24-Myr-average) seafloor spreading rates, shown as filled circles, were determined as follows: for each well-surveyed Southwest Indian Ridge spreading segment, we aggregated the DMS15 identifications of Chrons 1n, 2n, 2An.1, 2An.3, 3n.1 and 3n.4 from both sides of the ridge. Using standard methods for reconstructing magnetic reversals and fracture zones, we then found the best opening distance for each reversal and segment. We then corrected each opening distance for either 5 or 2 km of outward displacement, depending on its location along the ridge (DeMets *et al.* 2015), and inverted the sequence of corrected opening distances for each segment to find the best segment opening rate. Transform fault azimuths in (B) are from DeMets *et al.* (2010). Abbreviations: OD, outward displacement.

Ridge seafloor spreading velocities using angular velocities from the recently published Saria *et al.* (2014) and Kreemer *et al.* (2014) GPS studies. The former authors use the velocities of more than 100 continuous and campaign GPS stations on the Nubia, Lwandle, Somalia and Antarctic plates (locations shown in Fig. 1) to determine angular velocities that specify the instantaneous relative motions between these four plates (the angular velocities labeled 'GPS Only' from their table 3). The latter authors determine Nubia-Somalia-Antarctic plate angular velocities from 21 sites on the three plates (Fig. 1). We also use more recently determined velocities based on our own GPS data processing for 70 Nubia plate GPS sites, 18 Somalia plate sites and 19 sites on the Antarctic plate to determine the sensitivity of the geodetic estimates of Nubia-Somalia-Antarctic plate angular velocities to subsets of the underlying GPS site velocities. The Supporting Information provides more information about these GPS site velocities, including a summary of the processing methods for their underlying GPS observables, and information about the fits and weighted rms misfits of their best-fitting angular velocities.

Over geological timescales, we use data, angular velocities and finite rotations from two studies. From inversions of ~5000 identifications of magnetic reversals Chron 1n (0.78 Ma) through Chron 6 (19.7 Ma) and several thousand crossings of Southwest Indian Ridge transform faults and fracture zones, DeMets *et al.* (2015) estimate Nubia-Antarctic, Lwandle-Antarctic and Somalia-Antarctic rotations for 21 times since 20 Ma. Here, we use the subset of their data, rotations and angular velocities that span the past 5.24 Myr. In particular, we use the DMS15 noise-reduced rotations and angular velocities, which were determined from their noisier best-fitting finite-rotation sequences using a trans-dimensional, hierarchical Bayesian methodology (Iaffaldano *et al.* 2014).

Spanning the past 3.16 Myr, we use angular velocities and data from the MORVEL global plate motion study (DeMets *et al.* 2010). The MORVEL Nubia-Antarctic, Lwandle-Antarctic and Somalia-Antarctic angular velocities are constrained by more than one hundred 3.16-Myr-average seafloor spreading rates and 12 transform fault azimuths from the Southwest Indian Ridge and are also constrained to consistency with plate-circuit closures imposed by numerous kinematic data from other plate boundaries. The MORVEL data used here are limited to spreading rates and transform fault azimuths from the Nubia-Antarctic-Sur and Somalia-Antarctic-Capricorn three-plate circuits.

3 OUTWARD DISPLACEMENT

Near-bottom magnetic surveys of oceanic crust show that the normally and reversely magnetized bands of crust that give rise to the striped magnetic anomaly pattern adjacent to the mid-ocean ridges are separated by 1–5 km wide zones where the seafloor has mixed

magnetic polarities (e.g. Atwater & Mudie 1973; Macdonald 1977; Sempere *et al.* 1987). The widths of these magnetic reversal transition zones are determined by multiple processes that include the finite amount of time that is required for Earth's magnetic field to complete a reversal, the extrusion and intrusion of younger lavas onto and into pre-existing seafloor of opposite magnetization, extensional faulting across reversal boundaries and sloping reversal boundaries (Sempere *et al.* 1987). Each of these processes shifts the midpoint of a reversal transition zone away from the ridge relative to the idealized location for an instantaneously recorded field reversal, thereby defining the phenomenon known as outward displacement. Horizontal contraction of young seafloor via thermal cooling may also shift a reversal outward from its idealized location, further enhancing outward displacement (Kumar & Gordon 2009).

In situ, near-bottom surveys of magnetic reversal transition zones directly constrain their half-widths to 0.5–2.5 km (Sempere *et al.* 1987), thereby implying that the midpoints of two same-age magnetic reversals on either side of a mid-ocean ridge are 1–5 km farther apart than the idealized reversals of the same age. Regressions of seafloor ages and opening distances reconstructed from well-mapped magnetic reversals along seven seafloor spreading centres similarly indicate that magnetic reversal boundaries are consistently shifted 0.5–2.5 km outward from the ridge relative to their idealized, reconstructed locations (DeMets & Wilson 2008). The former, direct estimates of reversal zone transition half-widths and latter, indirect estimates agree well. Plate rotations that are determined by reconstructing seafloor spreading magnetic reversals thus require a modest correction for outward displacement in order to reveal the true plate motion. DeMets & Wilson (2008) estimate a best average correction of ≈2 km for most spreading centres.

Indirect estimates of the magnitude of outward displacement along the Southwest Indian Ridge from reconstructions of young magnetic reversals at 19 well-surveyed locations along the ridge range from 1.9 ± 0.3 km along the eastern two-thirds of the ridge to 5 ± 0.2 km along the western, Nubia-Antarctic segment of the ridge (DeMets *et al.* 2015). The former estimate is close to the 2 km global average reported by DeMets & Wilson (2008), whereas the latter is similar to well-determined 6–7 km transition zone widths along the densely surveyed Reykjanes Ridge south of Iceland (Sempere *et al.* 1990; DeMets & Wilson 2008; Merkouriev & DeMets 2008; 2014). Direct measurements of reversal transition zone widths for the Southwest Indian Ridge are unavailable. DeMets *et al.* (2010) corrected all Southwest Indian Ridge spreading rates that were used to estimate the MORVEL angular velocities for an assumed 2 km of outward displacement, equal to the global average reported by DeMets & Wilson (2008).

4 RESULTS

Our principal objectives are to jointly evaluate the steadiness of motion along the Nubia-Antarctic, Lwandle-Antarctic and Somalia-Antarctic plate boundaries during the past several million years and test whether the magnitude of outward displacement along the Nubia-Antarctic plate boundary is ≈5 km, as estimated by DMS15, or closer to the 2 km global average estimated for the remainder of the Southwest Indian Ridge and most other seafloor spreading centres. In order to accomplish these goals, we compare geodetic estimates of Nubia-Antarctic, Lwandle-Antarctic and Somalia-Antarctic plate motions to the DMS15 and MORVEL geological estimates. The geodetic estimates are unbiased by outward displacement, but are susceptible to other sources of systematic error. The geological estimates are affected by outward displacement, but are immune to various sources of systematic error that can affect GPS-derived angular velocities. The potential effects of various sources of systematic error on our results and conclusions are examined in Section 5.

4.1 Nubia-Antarctic plate motion

4.1.1 Comparison of geodetic and DMS15 estimates

Fig. 3(A) compares Nubia-Antarctic seafloor opening rates at a central location along the plate boundary as estimated with the DMS15 and MORVEL angular velocities, which span geological time intervals, and the Kreemer *et al.* (2014) and Saria *et al.* (2014) GPS-derived angular velocities, which give the instantaneous plate motion. The spreading rates estimated with the DMS15 angular velocities, which span nine time intervals between 7.5 Ma and the present (from Supporting Information Table S4 from DMS15), have averaged 14.0 mm yr^{-1} since 7.5 Ma and have varied by less than ±0.5 mm yr^{-1} since 5.2 Ma. The interval rates for times from 7.5 to 0.78 Ma are insensitive to the magnitude of the 5 km correction for outward displacement since the correction cancels nearly completely when the DMS15 finite rotations are differentiated to estimate the interval angular velocities. The evidence for steady motion between 7.5 and 0.78 Ma is thus robust. In contrast, the DMS15 angular velocity for the period 0.78 Ma to the present is sensitive to the 5 km correction that DMS15 applied to compensate for outward displacement of the Brunhes–Matuyama reversal. For example, if we recalibrate the DMS15 0.78 Myr to present angular velocity for outward displacement of 2 km rather than 5 km, equal to the global average correction that was applied for the MORVEL analysis, the modified Nubia-Antarctic opening rates estimated for the past 0.78 Myr increase by ∼40 per cent relative to the DMS15 estimate and imply an implausible ∼40 per cent acceleration with respect to the average opening rate from 7.5 to 0.78 Ma.

The GPS-derived angular velocities from Kreemer *et al.* (2014) and Saria *et al.* (2014) give respective opening rates of 14.0 ± 0.2 and 13.7 ± 0.3 mm yr^{-1} (blue and pink bars in Fig. 3A), within 2 per cent of the 14.0 mm yr^{-1} average opening rate estimated from the DMS15 angular velocities. The close agreement between the geodetic and DMS15 geological estimates suggests that the plate motion has been steady since at least 5.2 Myr and that outward displacement along the Nubia-Antarctic plate boundary averages ≈5 km.

Both GPS-derived angular velocities also fit the Nubia-Antarctic transform fault azimuths within their uncertainties (Fig. 2B). This suggests that both geodetic pole locations are accurate. The good fits to the transform fault azimuths can be used to estimate an approximate upper limit for any systematic biases that may affect the two geodetic angular velocity estimates. If we adopt ±1° as the maximum systematic misfit of the geodetic angular velocities to the transform fault azimuths (Fig. 2B), the corresponding limit for any systematic bias in the plate velocity component that is locally orthogonal to the transform faults is only ±0.25 mm yr^{-1}. Similarly, a simple visual comparison of the geodetic and DMS15 estimates for the plate motion component perpendicular to the ridge (i.e. the spreading rate) suggests an approximate upper limit for any systematic difference of ±0.5 mm yr^{-1} (Fig. 2A). Together, these suggest that potential systematic biases in the geodetic angular velocities due to factors such as drift of Earth's origin in ITRF2008 (Wu *et al.* 2011), postglacial rebound at stations in Antarctica (Argus *et al.*

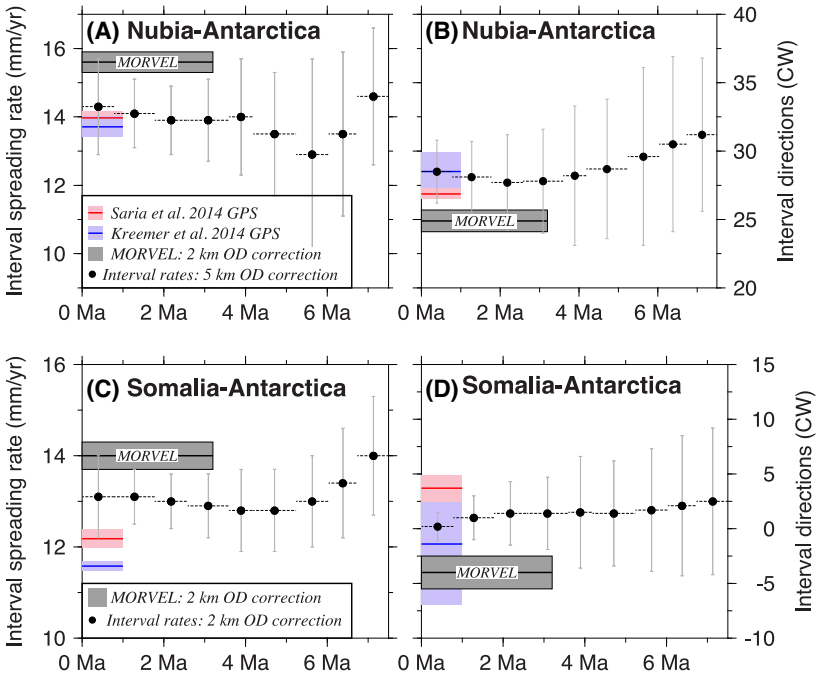

Figure 3. (A) Nubia-Antarctic interval spreading rates and (B) directions estimated at 52.8°S, 20.0°E and (C) Somalia-Antarctic interval spreading rates and (D) directions estimated at 31.6°S, 58.0°E, near the midpoints of their respective plate boundaries. Nubia-Antarctic and Somalia-Antarctic interval angular velocities from tables S4 and S6 of DeMets *et al.* (2015) are used to estimate the interval rates and directions (filled circles) and their 1σ uncertainties (vertical bars) and are corrected for 5 and 2 km of outward displacement (OD), respectively. Horizontal dashed lines define the period spanned by each stage velocity. Grey bars are centred on the 3.16-Myr-average plate velocities estimated with the MORVEL Nubia-Antarctic and Somalia-Antarctic angular velocities, both of which are corrected for 2 km of outward displacement (DeMets *et al.* 2010). The red and blue lines and their associated shaded areas show the relative plate velocities and 1σ uncertainties estimated with the Saria *et al.* (2014) and Kreemer *et al.* (2014) GPS-derived angular velocities.

2011; King *et al.* 2016), and the viscoelastic effects of nearby or distant earthquakes (Pollitz *et al.* 1998; King & Santamaria-Gomez 2016) are unlikely to exceed $\pm$1 mm yr^{-1} along the Nubia-Antarctic plate boundary.

4.1.2 *Comparison of MORVEL and DMS15 estimates*

Nubia-Antarctic opening rates estimated with the 3.16-Myr-average MORVEL angular velocity are $\approx$1.5 mm yr^{-1} faster than the DMS15 geological estimates for the past 5 Myr and 1–1.5 mm yr^{-1} faster than the GPS-derived opening rates (Figs 2A and 3A). Approximately 70 per cent of the difference between the DMS15 and MORVEL geological opening rate estimates is attributable to the 5 km correction for outward displacement that is implicit in the DMS15 estimate versus the 2 km correction that was applied for the MORVEL analysis. Differences in the data and methodologies that were used in the two studies are responsible for the remaining $\approx$0.5 mm yr^{-1} difference between the two geological estimates. The opening rates estimated with the DMS15 angular velocities are based on reconstructions of six magnetic reversals younger than 5.3 Ma, whereas the MORVEL opening rates are determined solely from Anomaly 2A. It thus seems likely that the DMS15 estimates are more accurate.

4.1.3 *Non-closure estimate around the Bouvet triple junction*

Measurements of seafloor opening rates and directions from the Mid-Atlantic Ridge south of 47 °S, corresponding to the Nubia-Sur plate boundary, and from the American-Antarctic Rise, which accommodates movement between Antarctic and Sur plates, provide useful, independent information about Nubia-Antarctic plate motion via closure of the Nubia-Antarctic-Sur plate circuit around the Bouvet Triple Junction. In the MORVEL analysis, this three plate circuit has the second largest non-closure of any three-plate circuit (DeMets *et al.* 2010), equivalent to a 3.3 $\pm$ 0.5 mm yr^{-1} linear velocity of circuit non-closure at the Bouvet Triple Junction (Case 1 in Fig. 4E). The probability that random errors in the MORVEL data are responsible for the large circuit non-closure is only 2 $\times$ 10^{-6} (DeMets *et al.* 2010). Plate non-rigidity, systematic data biases, or an incorrect calibration for outward displacement are thus more likely than random errors to be the source of the circuit non-closure. Based on evidence that the magnitude of the circuit non-closure diminishes for progressively larger, assumed values of outward displacement, DeMets *et al.* (2010) speculate that outward displacement along one or more of the three spreading centres that intersect at the Bouvet Triple Junction may be larger than the 2 km correction they assumed for their analysis.

If a systematic bias in the MORVEL Nubia-Antarctic rates is responsible for some of the circuit non-closure described above, then substituting seafloor opening rates that are estimated from the numerous DMS15 data and calibrated for 5 km of outward displacement should reduce the circuit non-closure. To evaluate this hypothesis, we estimated seafloor spreading rates for five well-surveyed spreading segments along the Nubia-Antarctic plate boundary from opening distances that we reconstructed for each spreading segment from the numerous DMS15 identifications of Chrons 1n, 2n, 2An.1, 2An.3, 3n.1 and 3n.4. The newly estimated opening rates span the past 5.24 Myr, during which the plate motion has been steady within uncertainties (Figs 2 and 3). Each 5.24-Myr-average opening rate

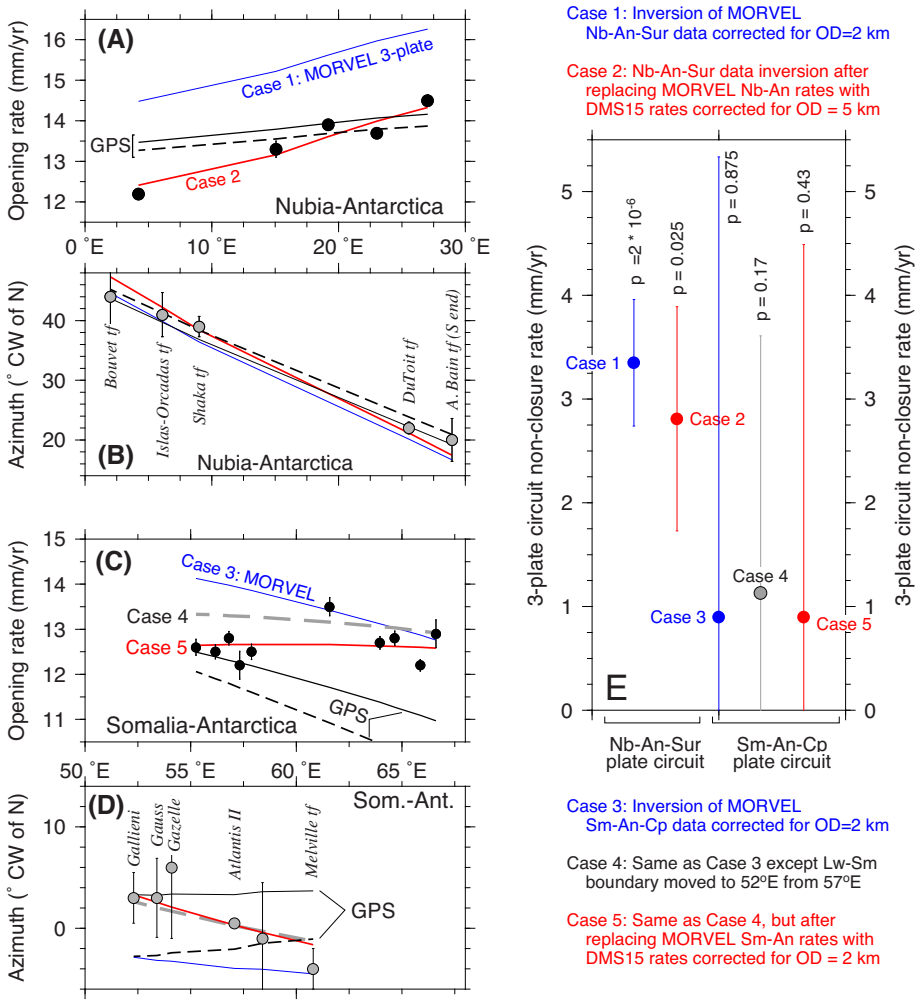

Figure 4. Effects of 5.2-Myr-average seafloor spreading rates from Fig. 3(A) and the assigned location of the Lwandle-Somalia plate boundary on closures of the Nubia-Antarctic-Sur (Nb-An-Sur) and Somalia-Antarctic-Capricorn (Sm-An-Cp) 3-plate circuits. (A) and (B) show fits of MORVEL (blue line), GPS (Saria *et al.* 2014, solid black line; Kreemer *et al.* 2014, dashed black line) and two alternative models (Cases 1 and 2 described in figure and text) to Nubia-Antarctic rates and azimuths. (C) and (D) show fits of MORVEL (blue line), GPS (Saria *et al.* 2014, solid black line; Kreemer *et al.* 2014, dashed black line) and three alternative models (Cases 3–5 described in figure and text) to Somalia-Antarctic rates and azimuths. Rates and azimuths are taken from Fig. 3. (E) Plate-circuit non-closures for Cases 1 and 2 (Nb-An) and Cases 3–5 (Sm-An) are determined in two ways. The fits to data from the Nb-An-Sur and Sm-An-Cp three-plate circuits from inversions that alternatively enforce and do not enforce circuit closure are compared via the F-ratio test (Gordon *et al.* 1987) to determine the probability p that the circuit non-closure is caused by random errors in the data. Probability values smaller than 0.01 indicate circuit non-closures that are significant at more than the 99 per cent confidence level. The same inversions are used to find an angular velocity of non-closure for each plate circuit, which is used to calculate a linear velocity of non-closure and its 1σ uncertainty at the Bouvet triple junction for the Nb-An-Sur circuit and the Rodriguez triple junction for the Sm-An-Cp circuit. Data that better satisfy plate-circuit closure give rise to smaller linear velocities of non-closure. Abbreviations: DeMets *et al.* (2015): DMS15; OD: outward displacement.

(black circles in Figs 3A and 4A) was constrained to consistency with outward displacement of 5 km and was assigned a standard error of ± 0.2 mm yr^{-1}, sufficient to give it high importance in the ensuing data inversion.

We inverted the MORVEL plate kinematic data from the Nubia-Antarctic-Sur plate circuit, including the five newly estimated Nubia-Antarctic spreading rates but excluding all of the MORVEL Nubia-Antarctic spreading rates, to find closure-enforced angular velocities for all three plate pairs. On average, the spreading rates determined with the newly estimated Nubia-Antarctic angular velocity are $\sim$2 mm yr^{-1} slower than the rates estimated from the original MORVEL data (compare blue and red lines in Fig. 4A). Encouragingly, the linear velocity of circuit non-closure at the Bouvet Triple Junction for the modified data, 2.8 ± 1.1 mm yr^{-1} (Case 2 in Fig. 4E), is 20 per cent smaller than the 3.4 ± 0.6 mm yr^{-1} linear velocity of circuit non-closure for the unmodified MORVEL data (Case 1 in Fig. 4E). The significance level of the circuit non-closure as measured with an F-ratio test is 97.5 per cent, below the 99 per cent threshold often applied when testing for plate-circuit non-closure (Gordon *et al.* 1987). By implication, the modified kinematic data from this three-plate circuit are more consistent with each other than was the case for the MORVEL observations.

As is shown in Figs 4(A) and (B), seafloor opening rates and directions that are estimated with the Nubia-Antarctic angular velocity determined from the modified three-plate inversion described above are more consistent with the rates and directions estimated with the Saria *et al.* (2014) and Kreemer *et al.* (2014) GPS angular velocities than with the MORVEL Nubia-Antarctic angular velocity.

We conclude that substituting the new, slower DMS15 Nubia-Antarctic seafloor spreading rates into the MORVEL data set has

three salutary effects. First, it reduces the magnitude and significance of non-closure around the Bouvet Triple Junction relative to those reported by DeMets *et al.* (2010). Second, it gives rise to more consistent geodetic and geological estimates of Nubia-Antarctic plate motion (Figs 4A and B). Finally, it suggests that Nubia-Antarctic plate motion has not changed significantly since at least 5.2 Ma (Fig. 3A).

4.2 Lwandle-Antarctic plate motion

A comparison of geological and geodetic estimates for the Lwandle-Antarctic plate pair, which share a boundary between 32°E and 52°E along the Southwest Indian Ridge, is less instructive than for the Nubia-Antarctic and Somalia-Antarctic plate pairs because relatively few geodetic measurements sample the motion of the Lwandle plate. We nonetheless include it for completeness. The DMS15 analysis suggests that Lwandle-Antarctic seafloor spreading rates have been steady since at least 5.24 Ma and that outward displacement averages 2 km, the same as was assumed for the MORVEL analysis of Lwandle-Antarctic plate motion.

4.2.1 Comparisons to the GPS estimate

The Lwandle-Antarctic opening rates estimated with the DMS15 5.24 Ma finite rotation are 0.5–1 mm yr^{-1} faster than those estimated with the Saria *et al.* (2014) GPS angular velocity (Fig. 2A). Given that Saria *et al.* (2014) used velocities from only two Lwandle plate GPS sites to estimate Lwandle plate motion, we consider it premature to interpret this difference as significant.

The opening rates estimated with the 3.16-Myr-average MORVEL Lwandle-Antarctic angular velocity are 1.5 mm yr^{-1} faster than the GPS-derived rates (Fig. 2A). The DMS15 opening rates thus agree more closely with the geodetic estimate than do the MORVEL opening rates. Given that the DMS15 Lwandle-Antarctic rotations were estimated from roughly twice as many data as was the MORVEL angular velocity, the superior agreement between the DMS15 and geodetic estimates is not unsurprising.

4.2.2 Comparison of the DMS15 and MORVEL estimates

The MORVEL and DMS15 estimates of Lwandle-Antarctic opening rates differ by a statistically insignificant 0.5 ± 0.6 mm yr^{-1} (95 per cent uncertainty) at the western end of the plate boundary and 1.0 ± 0.8 mm yr^{-1} at the eastern end of the boundary (Fig. 2A). Given that plate-circuit closures do not affect the Lwandle-Antarctic angular velocities estimated in either study and that both studies calibrated their Lwandle-Antarctic angular velocities for 2 km of outward displacement, the differences between the two must be caused by the different observations and methods that were used in the two studies to determine their Lwandle-Antarctic angular velocities and the assumption by DeMets *et al.* (2010) that the Lwandle-Somalia plate boundary intersects the Southwest Indian Ridge near 47°E versus 52°E for the DMS15 study.

4.3 Somalia-Antarctic plate motion

4.3.1 Comparison of geodetic and DMS15 estimates

Fig. 3(C) compares seafloor opening rates at a central location along the Somalia-Antarctic segment of the Southwest Indian Ridge as estimated with the following: (1) GPS-derived angular velocities from Kreemer *et al.* (2014) and Saria *et al.* (2014); (2) the 3.16-Myr-average MORVEL angular velocity; (3) nine DMS15 angular velocities that span intervals from 7.5 Ma to the present (Supporting Information Table S6 from DMS15). The high-resolution sequence of the DMS15 angular velocities indicate that the interval rates have averaged 13.0 mm yr^{-1} since 6.0 Ma and have varied by less than ±0.2 mm yr^{-1} during this time. The DMS15 angular velocities further indicate that the plate slip directions have remained steady since 6.0 Ma (Fig. 3D).

The opening rates we determined with both of the GPS-derived Somalia-Antarctic angular velocities are 1.0–1.4 mm yr^{-1} slower than the DMS15 estimates (Fig. 3C), in conflict with the plate kinematic evidence that Somalia-Antarctic motion was steady from 6 Ma to the present. In addition, the directions estimated with both GPS angular velocities misfit the azimuths of the Melville and Atlantis II transform faults (Figs 2B and 4D), which are estimated from multibeam surveys (Dick *et al.* 1991; D. Sauter, private communication, 2013). These differences suggest that the GPS angular velocities are either inaccurate or that Somalia-Antarctic plate motion has changed during the past 0.78 Ma. We evaluate this difference in more detail in Section 5.3.

Despite our concerns about possible inaccuracies in both GPS estimates of Somalia-Antarctic plate motion, the better agreement between the DMS15 estimate and the two GPS estimates than for the MORVEL estimate suggests that the DMS15 rotations more accurately describe the geologically recent motion between these two plates. We next compare the DMS15 and MORVEL estimates in more depth and in the context of their consistency with closure of the Somalia-Antarctic-Capricorn plate circuit.

4.3.2 The MORVEL and DMS15 estimates and closure around the Rodrigues Triple Junction

We explored the cause and significance of the differences between the DMS15 and MORVEL estimates of Somalia-Antarctic plate motion in two stages. We first examined how the different locations that are assumed in the two studies for the western boundary of the Somalia plate influence the estimated plate motion and plate-circuit closure. This topic is particularly relevant given that the MORVEL angular velocity fits all of the spreading rates and transform fault azimuths that are located east of 60°E (Figs 2, 4C and D), but misfits all of the observations west of 60°E. Part or all of this pattern of misfits may be related to the assumption by DeMets *et al.* (2010) that the Somalia plate extends no farther west than the Atlantis II transform fault at 57°E. In contrast, DMS15 assume that the undeformed Somalia plate extends as far west as the Gallieni transform fault at 52°E. In the second stage of the analysis, we evaluated the effects of substituting opening rates estimated from the DMS15 observations for the original MORVEL Somalia-Antarctic opening rates. To prepare for this part of the analysis, we estimated 5.24-Myr-average opening rates for 10 well-surveyed spreading segments between 52°E and 67°E from linear regressions of opening distances that we reconstructed for each spreading segment from 845 DMS15 identifications of Chrons 1n, 2n, 2An.3, 2An.3, 3n.1 and 3n.4 (Figs 2A and 4C). The best-fitting rates were constrained to consistency with outward displacement of 2 km and assigned uncertainties of ±0.2 mm yr^{-1}, sufficient to give them high importances in the ensuing data inversion.

The original MORVEL observations from the Somalia-Antarctic-Capricorn plate circuit consist of 102 seafloor spreading rates and transform fault azimuths from the Central Indian Ridge and western

500 km of the Southeast Indian Ridge and twenty-nine 3.16-Myr-average spreading rates and two transform fault azimuths from the Southwest Indian Ridge east of and including the Atlantis II transform fault (57°E). From these observations, DeMets *et al.* (2010) report a 0.9 ± 4.5 mm yr^{-1} linear velocity of non-closure for this three-plate circuit at the Rodrigues Triple Junction (shown as Case 3 in Fig. 4 E). The original MORVEL data satisfy closure of this plate circuit within their uncertainties.

We tested how the assumed location for the western boundary of the Somalia plate affects the plate-circuit closure by adding thirteen Southwest Indian Ridge spreading rates and four transform fault azimuths from locations between 52°E and 57°E from Supporting Information table 1 of DeMets *et al.* (2010) to the original 133 MORVEL data from the Capricorn-Somalia-Antarctic plate circuit and inverting the augmented data to find revised, closure-enforced angular velocities for all three plate pairs in the plate circuit. The revised Somalia-Antarctic angular velocity fits the 5.24-Myr-average rates determined from the DMS15 reversal identifications better than does the MORVEL angular velocity (compare the fits for Cases 3 and 4 in Fig. 4C) and fits the transform fault azimuths significantly better than does MORVEL (Fig. 4D).

The revised linear velocity of non-closure at the Rodrigues Triple Junction, 1.1 ± 2.5 mm yr^{-1} (Case 4 in Fig. 4 E), is larger than the 0.9 ± 4.5 mm yr^{-1} velocity of non-closure associated with the assumed MORVEL boundary location of 57°E (Case 3 in Fig. 4 E). The non-closure of the three-plate circuit is however statistically insignificant ($p = 0.17$, Fig. 4 E) as measured via an F-ratio comparison of the summed misfits of the best-fitting angular velocities for the three-circuit plate pairs to the misfit of the closure-enforced angular velocities. The improvements in fit to the Somalia-Antarctic plate kinematic data that are described in the previous paragraph are thus achieved without significantly degrading the fits to data elsewhere within the closure-enforced three-plate circuit. The DMS15 Somalia plate geometry is thus compatible with the MORVEL plate kinematic data.

We next substituted the ten 5.24-Myr-average Southwest Indian Ridge spreading rates described above for the MORVEL Somalia-Antarctic rates and inverted them with all six Southwest Indian Ridge transform fault azimuths east of and including the Gallieni transform fault (Fig. 4D) and all 102 MORVEL seafloor spreading rates and transform fault azimuths from the Capricorn-Somalia and Capricorn-Antarctic plate boundaries. The closure-enforced Somalia-Antarctic angular velocity from the inversion fits the 5.24-Myr-average spreading rates and the six transform fault azimuths well (Case 5 in Figs 4C and D). The plate-circuit non-closure at the Rodrigues Triple Junction, 0.9 ± 3.6 mm yr^{-1} (Case 5 in Fig. 4E), is unchanged from that reported by DeMets *et al.* (2010). An F-ratio comparison of the summed least-squares misfits for the three best-fitting angular velocities to the misfit of the closure-enforced angular velocities indicates that the probability is only 43 per cent that the circuit non-closure is statistically significant. The good fits to the modified Somalia-Antarctic data are thus achieved without significantly degrading the fits to the high-quality observations from the Capricorn-Somalia or Capricorn-Antarctica plate boundaries. An even better fit occurs if we invert the same observations while assigning a boundary location at 57°E, as assumed for the MORVEL analysis. For this model, the circuit non-closure is only 0.4 ± 3.9 mm yr^{-1}, the Somalia-Antarctic opening rates are nearly the same as for the previous estimate (Case 5) and the slip directions are intermediate between the MORVEL and Case 5 estimates shown in Fig. 4(D).

Our analysis thus indicates that the Somalia plate geometry used by DMS15 and opening rates estimated from their numerous reversal identifications are consistent with the MORVEL closure constraints for the Somalia-Antarctic-Capricorn plate circuit. Either estimate is thus equally acceptable when compared on the basis of their consistency with closure of the Somalia-Antarctic-Capricorn plate circuit. Given the superior agreement between the GPS and DMS15 estimates of Somalia-Antarctic plate motion, we provisionally conclude that the DMS15 rotations more accurately represent geologically recent Somalia-Antarctic plate motion than does MORVEL. The principal remaining uncertainty is whether undeformed areas of the Somalia plate extend as far west as 52°E north of the ridge or whether diffuse plate boundary deformation occurs from 52°E to 57°E, such that any plate kinematic data from those areas are significantly biased with respect to Somalia-Antarctic plate motion.

5 DISCUSSION AND IMPLICATIONS

5.1 Nubia-Antarctic plate motion since ~6 Myr and sensitivity analysis

The DMS15 analysis indicates that little or no change in Nubia-Antarctic plate motion occurred from ≈5.2 to 0.78 Ma, but allows for two interpretations of motion during the past 0.78 Myr. The simpler interpretation is that the motion from 0.78 Ma to the present has remained the same as the motion from 5.2 to 0.78 Ma. This requires that outward displacement average 5 km between the Bouvet Triple Junction and Andrew Bain Fracture Zone. The following three arguments favour this possibility: (1) both geodetic estimates of the Nubia-Antarctic angular velocity give instantaneous opening rates that agree well with the DMS15 estimate, which is calibrated for 5 km of outward displacement (Figs 2A and 3A). Both however disagree with the MORVEL estimate, which is calibrated for only 2 km of outward displacement. (2) Both geodetic angular velocities fit the Nubia-Antarctic transform fault azimuths within their uncertainties (Fig. 2B), an indicator that the geodetic estimates are accurate, (3) correcting Nubia-Antarctic seafloor spreading rates for 5 km of outward displacement reduces significant non-closure of the Nubia-Antarctic-Sur three-plate circuit reported by DeMets *et al.* (2010) to statistically insignificant levels (Section 4.1.3).

The second, less plausible interpretation is that Nubia-Antarctic seafloor spreading rates accelerated by ≈40 per cent after 0.78 Ma relative to the spreading rates that prevailed from 5.2 to 0.78 Ma. This more complex scenario requires peculiar errors in the Saria *et al.* (2014) and Kreemer *et al.* (2014) Nubia-Antarctic angular velocities, such that the directions estimated with the angular velocities are accurate (Fig. 2B), but their estimated spreading rates are too slow by 1.5–2 mm yr^{-1} (Fig. 2A). We next briefly evaluate four possible sources of error in the geodetically derived angular velocities to test this seemingly implausible scenario.

5.1.1 Effect of random site velocity errors

We first consider whether random errors in the Nubia and Antarctic GPS site velocities that were used by previous authors could be responsible for the underestimated Nubia-Antarctic opening rates described above. To do so, we estimated our own, updated Antarctic-ITRF08, Nubia-ITRF08 and Nubia-Antarctica angular velocities (Table 1) from the velocities of 19 continuous GPS sites well

Table 1. GPS-derived angular velocities and uncertainties.

Plates	Latitude	Longitude	$\dot{\omega}$	Covariances					
	(°N)	(°E)	(° Myr^{-1})	σ_{xx}	σ_{xy}	σ_{xz}	σ_{yy}	σ_{yz}	σ_{zz}
AN-IGS08	59.17	234.14	0.221	1.86	0.34	− 0.66	2.50	− 2.95	18.34
NB-IGS08	49.12	278.46	0.267	2.64	0.77	− 0.88	0.77	− 0.36	0.89
SM-IGS08	49.42	265.77	0.310	34.73	33.48	− 7.51	38.80	− 7.67	5.77
AN-NB	− 5.72	138.60	0.124	4.51	1.12	− 1.54	3.26	− 3.31	1.92
AN-SM	− 20.58	115.29	0.129	36.59	33.82	− 8.16	41.30	− 10.62	24.11
NB-SM	− 33.83	34.40	0.059	37.37	34.26	− 8.39	39.57	− 8.03	6.66

Notes: These angular velocities describe rotation of the first listed plate relative to either IGS08 or the second listed plate. The IGS08 reference frame is constrained to evolve in a manner identical to ITRF08 (Altamimi *et al.* 2011), hence the angular velocities are the same as if ITRF08 were the geodetic reference frame. The angular rotation rate $\dot{\omega}$ has units of degrees per millions of years. Angular velocity covariance units are 10^{-10} rad^2 Myr^{-2}. Abbreviations: AN: Antarctic plate; NB: Nubia plate; SM: Somalia plate.

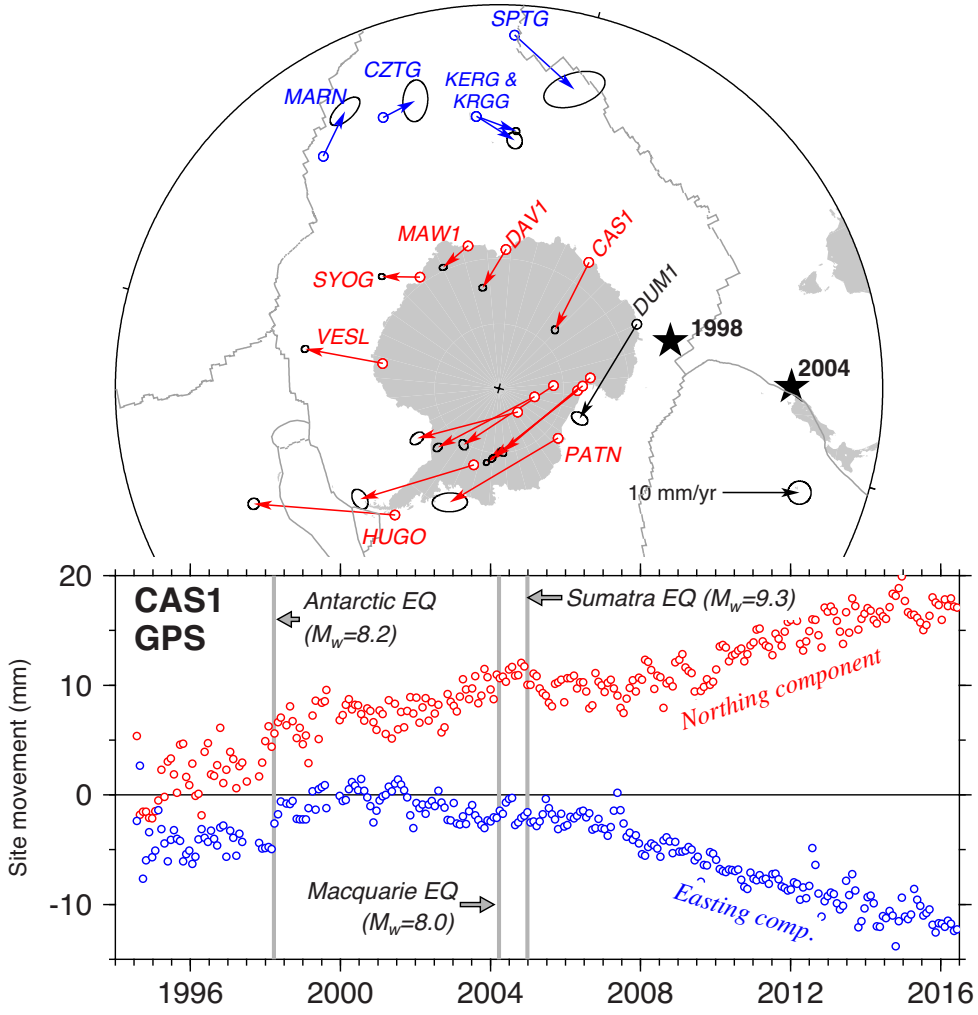

Figure 5. Antarctic GPS site velocities and 30 d average position time-series for site CAS1. Stars indicate the epicentres of the 1998 March 25 M = 8.2 Antarctic and 2004 March 23 M = 8.0 Macquarie Ridge earthquakes. The blue and red arrows show the velocities of the 5 oceanic island sites and 14 continental sites used for the sensitivity analysis. Velocities are relative to ITRF2008. Error ellipses are 1σ. The position time-series for site CAS1 shows the northing and easting changes in 30 d average site positions in millimetres with respect to the Antarctic plate interior. Obvious changes in the slopes of both components are variously caused by transient deformation triggered by the 1998 and 2004 earthquakes, possibly including the 2004 December 26 M = 9.3 Sumatra earthquake. The unlabeled Antarctic site velocities are for stations BRIP, DEVI, FALL, HOWN, MCM4, RAMG and ROB4.

distributed on the Antarctic plate (red and blue circles in Fig. 5 and Supporting Information Fig. S1) and 70 GPS sites well distributed in presumably undeforming regions of the Nubia plate (Supporting Information Fig. S2). Further information about the methods we used to process the original GPS data from these sites and estimate their velocities is found in the Supporting Information.

Opening rates that are estimated with the new Nubia-Antarctic angular velocity (shown by the bold blue-red dashed line in

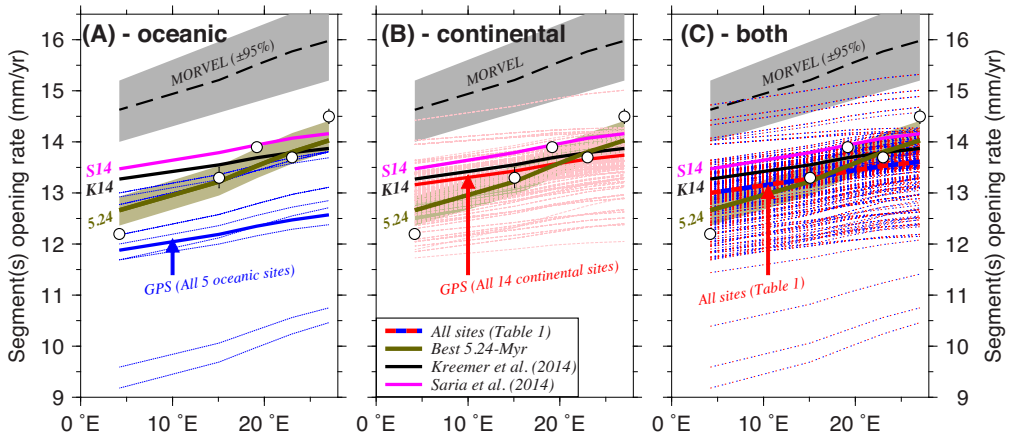

Figure 6. Sensitivity of GPS estimates of Nubia-Antarctic spreading rates to the GPS site velocities that are used to estimate Antarctic plate motion. The 19 Antarctic plate GPS site velocities selected for the analysis, consisting of five oceanic sites (blue) and 14 continental sites (red), are shown in Fig. 5. The thin blue and red lines shown, respectively, in panels A and B show all realizations of Nubia-Antarctic opening rates derived by inverting the velocities of 70 Nubia plate GPS sites with the azimuths of four transform faults from the Nubia-Antarctic plate boundary and all possible two-site combinations of the five oceanic GPS sites (panel A) or the 14 continental sites (panel B). Panel C repeats the analysis for all possible two-site combinations of the 19 Antarctic plate GPS velocities. The bold red, blue and red-blue lines in panels A, B and C (respectively) show the rates estimated from simultaneous inversions of all of the data. The dark green line and associated shaded area (labeled '5.24') show opening rates and their 1σ uncertainties estimated with a 5.24 Myr constant-motion angular velocity variously calibrated for 4–6 km of outward displacement. Opening rates estimated with the MORVEL 3.16 Ma (DeMets *et al.* 2010) and Kreemer *et al.* (2014) and Saria *et al.* (2014) GPS angular velocities are shown for comparison, as are 5.24-Myr-average opening rates determined directly from reversal crossings for five well-surveyed ridge segments (open circles).

Fig. 6C) differ by less than 0.5 mm yr^{-1} from rates estimated with the Kreemer *et al.* (2014) and Saria *et al.* (2014) angular velocities. The newly estimated opening rates fit the 5.24-Myr-average opening rates and four transform fault azimuths as well as or better than do the previous geodetic estimates (not shown). Like the previous geodetic estimates, our newly estimated geodetic rates are systematically slower than the MORVEL estimates by 1.5 mm yr^{-1} or more.

That three independent geodetic estimates of Nubia-Antarctic plate motion all give instantaneous opening rates that are 1.5–2 mm yr^{-1} slower than the MORVEL estimate suggests that it is unlikely that random errors in the GPS site velocities are responsible for the difference.

5.1.2 *Effect of possible origin drift in ITRF2008*

Another potential source of error in geodetic plate motion estimates is possible slow movement of Earth's centre of mass in the ITRF2008 geodetic reference frame (Argus 2007, 2012). Any motion of the frame origin, which is assumed to be stationary in ITRF2008 and earlier versions of ITRF, would systematically bias all GPS site velocities and hence all angular velocities estimated in ITRF2008. From an analysis of Gravity Recovery and Climate Experiment gravity measurements, 3-D geodetic site velocities in ITRF2008 and ocean bottom pressure measurements, Wu *et al.* (2011) estimate a $\pm$0.5 mm yr^{-1} upper limit for any drift of Earth's centre of mass in ITRF2008, with best drift estimates of -0.4 ± 0.1, -0.2 ± 0.1 and -0.5 ± 0.2 mm yr^{-1} in the *X*-, *Y*- and *Z*-directions, respectively.

We determined the sensitivity of geodetic estimates of Nubia-Antarctic seafloor spreading rates to possible origin drift in ITRF2008 as follows: we first adjusted the Cartesian velocity components of all 89 GPS sites on the Nubia and Antarctic plates for Wu *et al.*'s best drift rate estimates from the previous paragraph. We then inverted the 89 adjusted site velocities to find their best fitting, Nubia-Antarctic angular velocity and compared the opening rates estimated with the revised angular velocity to rates estimated assuming a stationary origin. The difference between the two sets of rates is only $\sim$0.1 mm yr^{-1}. This small difference indicates that the effects of origin drift on the Nubia-ITRF2008 and Antarctic-ITRF2008 angular velocities largely cancel each other when the two angular velocities are combined to find the Nubia-Antarctic angular velocity. This difference is too small to account for the $>$1.5 mm yr^{-1} discrepancy between the geodetic and MORVEL estimates. We thus reject possible drift of Earth's centre of mass in ITRF2008 as a source of significant error in the GPS estimates of Nubia-Antarctic plate motion that were considered in this study.

5.1.3 *Effect of glacial isostatic adjustment in Antarctica*

The isostatic effects of changes in Antarctic ice thickness, hereafter referred to as glacial isostatic adjustment or GIA, constitute a potential source of bias in Antarctic GPS site velocities (Argus *et al.* 2011; King *et al.* 2016). Based on their evaluations of 26 alternative GIA models, King *et al.* (2016) estimate the mean horizontal effects of GIA in Antarctica to range from 0.11 to 0.84 mm yr^{-1}. GIA could thus significantly bias GPS site velocities and hence Antarctic plate angular velocity estimates with respect to the underlying plate motion.

Given that the effects of GIA vary with location, geodetic estimates of the Nubia-Antarctic angular velocity will depend to varying degrees on the geography of the Antarctic plate sites that are used to estimate Antarctic plate motion. We approximated the sensitivity of Nubia-Antarctic angular velocities to possible geographic variations in the biases that affect Antarctic plate GPS site velocities by deriving Nubia-Antarctic angular velocities for all possible two-site combinations of the 19 Antarctic site velocities included in our analysis.

We first explored the sensitivity of the Nubia-Antarctic angular velocity to the velocities of the five oceanic island sites on the

Antarctic plate (blue arrows in Fig. 5), which should be relatively unaffected by GIA due to their distance from Antarctica. For each of the 10 possible two-site combinations of velocities for the five oceanic island sites, we combined and inverted the two-site velocities along with the 70 Nubia plate GPS site velocities and all four Nubia-Antarctic transform fault azimuths from the MORVEL data (the latter were included to encourage solutions that give geologically plausible opening directions along the Southwest Indian Ridge). We then used the Nubia-Antarctic angular velocity that best fit each set of observations to estimate instantaneous spreading rates along the Southwest Indian Ridge. The resulting rates, which vary from 9.5 to 13.5 mm yr^{-1} near the midpoint of the plate boundary (thin blue lines in Fig. 6A), are all significantly slower than the 14.5–16 mm yr^{-1} rates estimated with the MORVEL angular velocity. The velocity combinations that include either of the two GPS stations on Kerguelen Island give rise to the slowest opening rate estimates, that is, the estimates that are the least consistent with the DMS15 and MORVEL estimates. In contrast, the combinations that include either or both of the GPS sites on Marion or Crozet islands, which are the Antarctic plate GPS stations closest to the Southwest Indian Ridge, give rise to the fastest opening rates, that is, those that are the most consistent with the two geological estimates. This could be early evidence that the Antarctic plate deforms internally, such that the sites nearest the Southwest Indian Ridge provide the most reliable geodetic estimates of instantaneous movement across this feature.

We next repeated the analysis for all possible two-site combinations of the velocities of the 14 GPS sites on the Antarctic continent, where GIA effects should be larger than for the five oceanic sites. The resulting opening rates range from 12 to 15 mm yr^{-1} near the boundary midpoint (red dashed lines in Fig. 6B). With one exception, all of the numerous opening rate estimates are slower than the rates estimated with the MORVEL angular velocity, with an average difference of $\approx$2 mm yr^{-1}.

Finally, we repeated the analysis for all possible two-site combinations of the 19 oceanic and continental sites (thin blue-red dotted lines in Fig. 6C). Only three of the $\approx$150 spreading rate realizations fall partially within the 95 per cent uncertainty region for the opening rates estimated with MORVEL. The remaining estimates, which vary from 10 to 14.5 mm yr^{-1} at the midpoint of the plate boundary, are $\approx$2 mm yr^{-1} slower than the MORVEL estimate, but agree well with the 5.24-Myr-average rates estimated by DMS15.

Our updated GPS estimates of Nubia-Antarctic spreading rates thus differ insignificantly from the geological opening rate estimates for the past 5.24 Myr, but are uniformly slower than estimated with MORVEL. Biases in the geodetic estimates due to the influence of GIA in Antarctica thus do not appear to be capable of reconciling the difference between geodetic and the MORVEL estimates of Nubia-Antarctic plate motion.

5.1.4 Effect of earthquake viscoelastic rebound

Transient viscoelastic deformation triggered by the 1998 March 25 $M_w = 8.2$ Antarctica earthquake and possibly other earthquakes could also bias Antarctic GPS site velocities. King & Santamaria-Gomez (2016) show that the 1998 Antarctic earthquake triggered measurable transient deformation at continuous GPS site DUM1 in eastern Antarctica, roughly 600 km from the 1998 epicentre (site location shown in Fig. 5). Fig. 5 shows that the motion of GPS site CAS1, which is located nearly 2000 km from the earthquake epicentre, also changed after the 1998 earthquake. The change in motion at this distant site supports modeling results reported by King & Santamaria-Gomez (2016), which suggest that the earthquake's residual viscoelastic effects may still be as large as $\approx$1 mm yr^{-1} in much of Antarctica. If so, then viscoelastic rebound from the 1998 earthquake may cause horizontal site velocity biases that are comparable to or larger than GIA at many locations in Antarctica.

Given that the five oceanic island sites on the Antarctic plate are located 4800–6400 km from the 1998 earthquake, any residual viscoelastic effects of the 1998 earthquake at those sites should be less than few tenths of a millimetre per year (see fig. 3 in King & Santamaria-Gomez 2016). Despite the presumably minor effects of the 1998 earthquake on their station velocities, none of the Nubia-Antarctic angular velocities that were estimated from subsets of the velocities of the five oceanic sites on the Antarctic plate give seafloor spreading rate estimates that are as fast as those estimated by MORVEL (Fig. 6A). We thus consider it unlikely that viscoelastic rebound from the 1998 earthquake can account for the 1.5–2 mm yr^{-1} difference between the MORVEL and geodetic estimates of Nubia-Antarctic plate motion.

5.2 Somalia-Antarctic plate motion and sensitivity analysis

The inconsistencies shown in Fig. 2 between Somalia-Antarctic spreading rates and directions that are estimated from angular velocities derived from GPS measurements and from the DMS15 data and angular velocities have multiple possible causes that include the following: (1) a possible change in Somalia-Antarctic plate motion during the past 0.78 Myr. (2) A possible misidentification by DMS15 of the low-fidelity magnetic anomaly sequence at the eastern end of the Southwest Indian Ridge. (3) Inaccurate geodetic estimates of Somalia-Antarctic angular velocities due to some combination of random errors in the geodetic velocities, geodetic undersampling of Somalia plate motion, or systematic errors in the GPS site velocities due to drift of Earth's origin in ITRF2008, glacial isostatic adjustment in Antarctica and/or transient viscoelastic deformation triggered by large regional earthquakes (also see Section 5.1). We consider these briefly below.

Although we cannot disprove the possibility that Somalia-Antarctic seafloor spreading rates have slowed significantly since 0.78 Ma, a recent slowdown seems implausible given the evidence presented by DMS15 and described in Section 5.3 for steady Somalia-Antarctic opening rates between 6 and 0.78 Ma (also see Fig. 3C). We also consider it unlikely that misidentifications by DMS15 of one or more magnetic reversals along part or all of the Somalia-Antarctic plate boundary might be responsible for the difference between the DMS15 and geodetic estimates of Somalia-Antarctic seafloor spreading rates. Nine of the ten 5.24-Myr-average Somalia-Antarctic opening rates that we estimated from the DMS15 magnetic reversal crossings are the same within $\pm$0.5 mm yr^{-1} (Fig. 4C). This level of consistency is unlikely if one or more magnetic reversals were identified incorrectly along one or more of the 10 spreading segments for which we estimated the opening rates. It is also unlikely that the 5.24-Myr-average Somalia-Antarctic seafloor spreading rates would satisfy closure of the Capricorn-Somalia-Antarctic plate circuit (Section 4.3.2) if the rates were erroneous due to misidentified magnetic reversals.

Inaccuracies in the GPS angular velocities for the Somalia and/or Antarctic plates thus seem the likeliest cause for the misfits to the geological data. In particular, the poor fits of both geodetic estimates

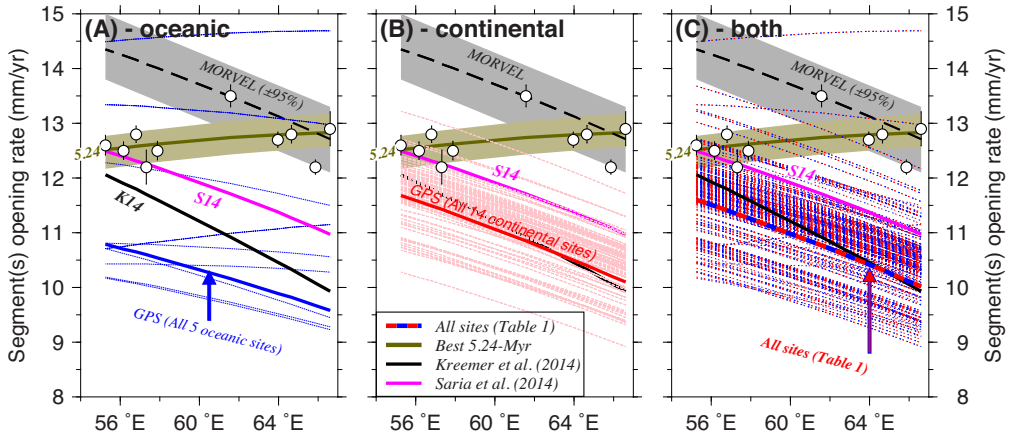

Figure 7. Sensitivity of GPS estimates of Somalia-Antarctic spreading rates to the GPS site velocities that are used to estimate Antarctic plate motion. The 19 Antarctic plate GPS site velocities selected for the analysis, consisting of five oceanic sites (blue) and 14 continental sites (red), are shown in Fig. 5. The thin blue and red lines shown, respectively, in panels A and B show all realizations of Somalia-Antarctic opening rates derived by inverting the velocities of 18 Somalia plate GPS sites with the azimuths of six transform faults from the Somalia-Antarctic plate boundary and all possible two-site combinations of the five oceanic GPS sites (panel A) or the 14 continental sites (panel B). Panel C repeats the analysis for all possible two-site combinations of the 19 Antarctic plate GPS velocities. The bold red, blue and red-blue lines in panels A, B and C (respectively) show the rates estimated from simultaneous inversions of all of the data. The dark green line and associated shaded area (labeled 'TS') show opening rates and their 1σ uncertainties estimated with a 5.24 Myr constant-motion angular velocity variously calibrated for 1–3 km of outward displacement. Opening rates estimated with the MORVEL 3.16 Ma (DeMets *et al.* 2010), and the Kreemer *et al.* (2014) and Saria *et al.* (2014) GPS angular velocities are shown for comparison, as are 5.24-Myr-average opening rates determined directly from reversal crossings for 10 well-surveyed ridge segments (open circles).

to the azimuths of the Melville and Atlantis II transform faults at the eastern end of the Southwest Indian Ridge (Fig. 2B) suggest that the geodetic estimates are inaccurate. We thus consider below the random and systematic errors that could affect the geodetic velocities.

5.2.1 Effect of random site velocity errors

We approximated the degree to which the geodetic estimates of Somalia-Antarctic plate motion may be influenced by differences between the sites that were selected to determine Somalia and Antarctic plate motions and the data that were used to determine each site velocity by comparing plate boundary velocities that we estimated with the Kreemer *et al.* (2014) and Saria *et al.* (2014) Somalia-Antarctic angular velocities and with an updated Somalia-Antarctic angular velocity (Table 1) determined from an inversion of our own velocities for 18 Somalia plate GPS sites (Supporting Information Fig. S3) and 19 Antarctic plate GPS sites (Fig. 5 and Supporting Information Fig. S1). The opening rates estimated with all three of these GPS-derived angular velocities differ by no more than 1 mm yr^{-1} along the plate boundary (Fig. 7C). All three geodetic estimates are slower than the corresponding DMS15 or MORVEL opening rate estimates, typically by more than 1 mm yr^{-1}. Given that the discrepancy between the MORVEL and geodetic opening rate estimates exceeds the scatter between the three geodetic estimates, it seems unlikely that the difference will be reconciled by selecting a different subset of stations to represent the motion of either plate or by extending the position time-series at the existing stations.

5.2.2 Effect of possible origin drift in ITRF2008

Adjusting the velocities of all 37 Somalia and Antarctic plate GPS sites for Wu *et al.*'s (2011) best estimates of the rate of ITRF08 origin drift (Section 5.1.2) and inverting the adjusted site velocities gives a modified, best-fitting angular velocity that predicts Somalia-Antarctic opening rates that are only ∼0.1 mm yr^{-1} different from the rates estimated using our newly determined best-fitting angular velocity (Table 1), which assumes that the ITRF2008 origin is stationary. Drift of the ITRF2008 origin thus cannot account for the discrepancy between the geodetic and geological estimates of Somalia-Antarctic plate motion.

5.2.3 Sensitivity to glacial isostatic adjustment in Antarctica

Borrowing methods that are described in Section 5.1.2, we approximated the sensitivity of the Somalia-Antarctic geodetic angular velocity to possible geographic variations in the GIA biases that affect the 19 Antarctic plate GPS sites included in our analysis. We inverted all possible two-site combinations of the 19 Antarctic plate site velocities with the 18 Somalia plate GPS site velocities and the azimuths of six Southwest Indian Ridge transform faults east of 52°E (DeMets *et al.* 2010). The latter azimuths were included to discourage angular velocity estimates that give implausible seafloor opening directions along the Southwest Indian Ridge.

Fig. 7 summarizes the results. The opening rates estimated with angular velocities based on two-site combinations of the GPS velocities for the five oceanic islands on the Antarctic plate vary widely (Fig. 7A). The velocity combinations that include either of the two GPS stations on Kerguelen Island give rise to opening rate estimates that are 2–3.5 mm yr^{-1} slower than the DMS15 and MORVEL estimates. In contrast, the combinations that include either or both of the GPS sites on Marion or Crozet islands give rise to faster opening rates that are consistent with the DMS15 and MORVEL estimates. Geodetic estimates of Southwest Indian Ridge motion may thus be the most reliable if they are based on the velocities of the two GPS stations nearest the Southwest Indian Ridge.

None of the numerous realizations of the Somalia-Antarctic opening rates that we estimated from two-station subsets of the 14 GPS stations on Antarctica were consistent with the MORVEL

estimate (Fig. 7B) and only three of the ≈150 geodetic spreading rate realizations were even partially consistent with the 5.24 Myr estimate based on the DMS15 data (Fig. 7B). We conclude that the differences between the geological and geodetic estimates of Somalia-Antarctic plate motion are largely robust with respect to the subset of the GPS site velocities that are used to estimate the Antarctic plate angular velocity, except for solutions that are based on the velocities of the GPS sites on Crozet and Marion islands near the Southwest Indian Ridge.

5.2.4 Effect of viscoelastic rebound from the 2004 Sumatra earthquake

Transient deformation triggered by the $M_w = 9.3$ 2004 Sumatra earthquake or previous earthquakes such as the 1998 $M_w = 8.2$ Antarctic intraplate earthquake (King & Santamaria-Gomez 2016) may bias geodetic estimates of Somalia-Antarctic plate motion, even at sites located far from the earthquakes. For example, the velocity of continuous GPS station DGAR on Diego Garcia ∼3000 km east of the Sumatra trench changed by 1.4 mm yr^{-1} toward N63°E (blue arrow in Fig. 8A) after the Sumatra earthquake with respect to the site's well-determined motion during the eight years before the earthquake (Fig. 8B). Modeling of the near-field post-seismic deformation measured after the 2004 Sumatra earthquake suggests that fault afterslip and viscoelastic mantle flow both contributed to deformation at sites near the rupture zone (Pollitz *et al.* 2006; Chlieh *et al.* 2007; Pollitz *et al.* 2008).

To our knowledge, no estimate of the post-seismic effects of the 2004 Sumatra earthquake has been published for locations much farther from the rupture zone, which are relevant to this study. We therefore applied Visco-1-D software (Pollitz 1997) to the Banerjee *et al.* (2007) slip solution for the Sumatra earthquake, which approximates the rupture with nine shallow- and intermediate-depth slip patches. We approximated the viscoelastic structure of the oceanic lithosphere and mantle using Pollitz *et al.*'s (2006) 'Rheology 1' structure, in which viscoelastic flow in oceanic regions is dominated by a low-viscosity asthenosphere with linear Maxwell rheology between depths of 62–220 km. In order to maximize the viscoelastic response estimated for the period late 2004 until early 2012, after which the motion at DGAR was further disrupted by the 2012 April 11 $M_w = 8.6$ Wharton Basin earthquake, we fixed the viscosity of the asthenosphere to 3×10^{18} Pa s, representing an approximate lower limit estimated by James *et al.* (2009) from modeling of sea level curves in Cascadia.

Fig. 8(A) shows the velocities estimated with the above viscoelastic model averaged over the 7.3-yr-long period between the 2004 Sumatra earthquake and 2012 $M_w = 8.6$ Indian Ocean earthquake. At site DGAR, the estimated viscoelastic deformation averages 0.5 mm yr^{-1} toward N57°E (red arrow in Fig. 8A), consistent with the N63°E change in direction measured at DGAR, but ≈1 mm yr^{-1} slower than the measured change of 1.4 mm yr^{-1}. The good agreement between the observed and modeled directions is consistent with the hypothesis that the earthquake triggered the velocity change shown in Fig. 8(B); however, the discrepancy between the modeled and observed rate change suggests that earthquake afterslip also contributed significantly to the deformation, even at locations as remote as Diego Garcia. Overall, the directions and magnitudes of the viscoelastic deformation vary significantly throughout the Indian Ocean basin, reflecting variations in the coseismic stress perturbations at different locations in the ocean basin and surrounding continents.

The observations and viscoelastic modeling thus clearly indicate that transient deformation associated with the 2004 Sumatra earthquake extended west to Diego Garcia, several hundred kilometres from the western boundary of the Somalia plate. Although our viscoelastic modeling suggests that similar post-seismic movement should also be observable at the continuous GPS stations REUN and SEY1 west of the Central Indian Ridge (located in Fig. 8), visual inspections of the time-series for both sites reveal no clear evidence for more rapid eastward motion after late 2004. Noise in those GPS time-series may preclude identifying any small changes in motion triggered by the earthquake. Alternatively, the Central Indian Ridge or possibly its sub-axial asthenosphere may decouple the Somalia plate from post-seismic deformation that affects the lithosphere and asthenosphere east of the Central Indian Ridge.

Absent any clear evidence for significant post-seismic deformation at locations on the Somalia plate, we provisionally conclude that its potential effect on our results is too small to alter any of our primary conclusions. We note however that it is premature to dismiss as unimportant the coseismic and viscoelastic effects of large regional earthquakes for estimating the regional plate motions. In addition to the 1998 Antarctic and 2004 Sumatra earthquakes considered herein, other earthquakes large enough to induce significant far-field post-seismic deformation may include the 2005 March Nias earthquake ($M_w = 8.7$), the 2007 September Sumatra trench earthquake ($M_w = 8.5$) and the 2012 April Wharton Basin ($M_w = 8.6$) earthquake. Their time-dependent effects depend on critical unknowns such as whether the mantle and/or asthenosphere are better approximated with linear Maxwell, Burgers body (e.g. Pollitz *et al.* 2008), or transient power-law rheologies (e.g. Freed *et al.* 2012), and whether the Indian Ocean seafloor spreading centres and their underlying asthenosphere perturb the viscoelastic deformation pattern.

5.3 Broader implications

If the MORVEL estimate of Nubia-Antarctic plate motion is too fast by 1–2 mm yr^{-1}, as suggested by DMS15 and the analysis presented herein (Fig. 2A), then this bias will affect the MORVEL estimates of motion for other plates that are embedded in plate circuits connected to the Nubia-Antarctic plate pair. For example, DeMets & Merkouriev (2016) show that Pacific-North America angular velocities that incorporate a 5 km calibration for outward displacement along the Nubia-Antarctic plate boundary predict geologically recent motion that is significantly closer to GPS estimates than does MORVEL. At the broadest level, efforts to use marine geophysical data to estimate recent plate motions with accuracies better than ±1 mm yr^{-1} must cope with hard-to-detect, systematic data biases that may vary with location (e.g. outward displacement) and data type. Similarly, geodetic plate velocities are susceptible to a wide range of potential systematic errors that must be considered during comparisons of geological and geodetic plate motion, including those treated above and others such as the cumulative effects on GPS site positions of small coseismic offsets from distant earthquakes (Tregoning *et al.* 2013).

5.4 Conclusions

A close agreement between Southwest Indian Ridge seafloor spreading rates estimated from newly published, detailed reconstructions of Nubia-Antarctic plate motion (DeMets *et al.* 2015) and from recently published GPS angular velocities (Kreemer *et al.*

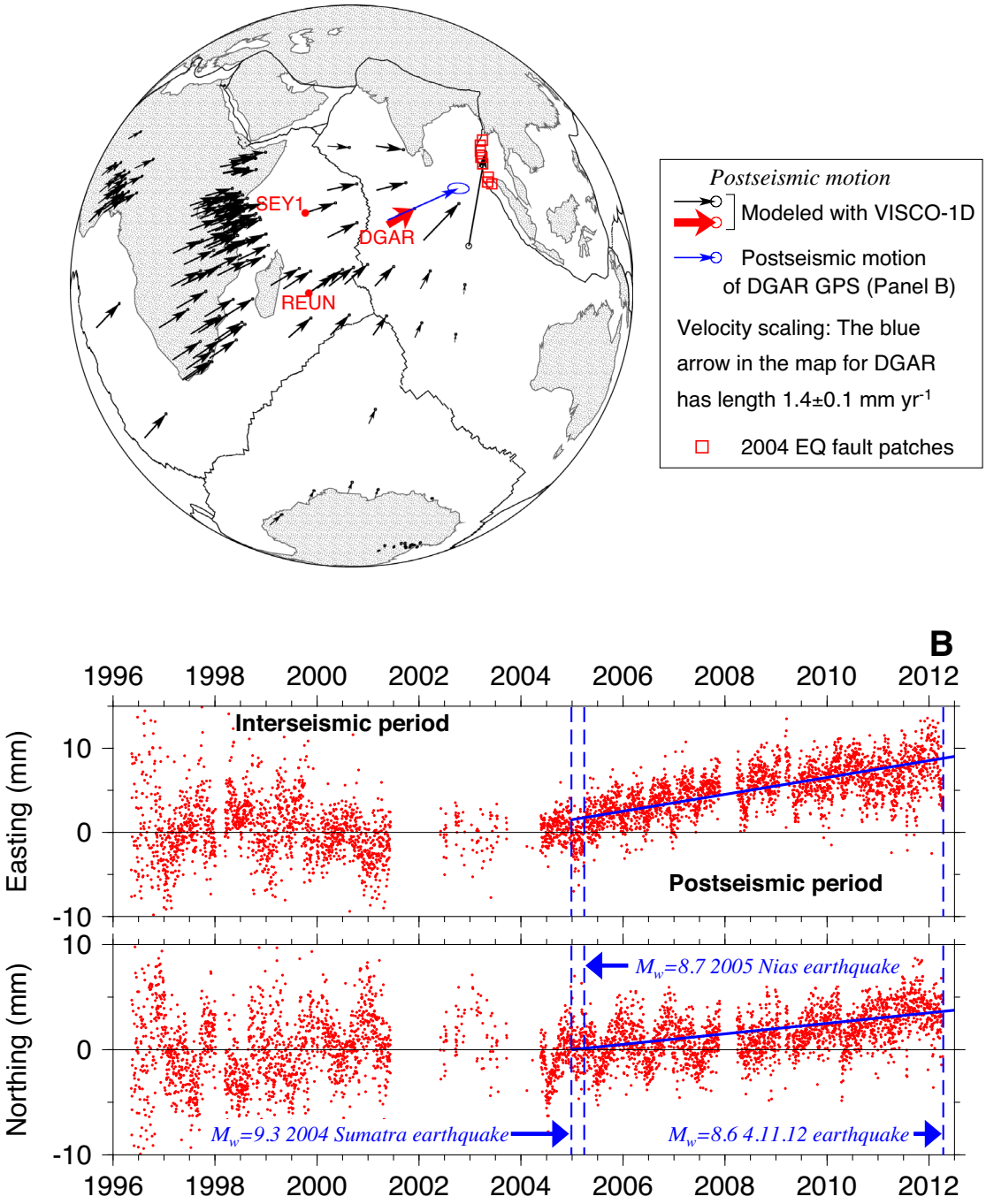

Figure 8. Effect of the M_w 9.3 2004 December 26 Sumatra earthquake on Diego Garcia GPS station DGAR. (A) Estimated regional velocity perturbations due to viscoelastic deformation triggered by the 2004 Sumatra earthquake versus the velocity change (blue arrow) recorded at DGAR for 2005.0–2012.25. Velocity perturbations are calculated for the period 2005.3 until the 2012 April 11 M_w 8.6 Wharton Basin earthquake. Details of the viscoelastic model are given in the text. Red squares mark the 2004 Sumatra earthquake slip patches that were used to estimate the viscoelastic response. (B) Daily easting and northing GPS positions for DGAR reduced by their best-fitting pre-earthquake slopes (1996.0–2004.98) and corrected by the movements during the 2004 earthquake. The blue lines that best fit the daily site positions after the earthquake clearly show eastward and northward accelerations of the site motion, in the same direction as, but faster than the accelerations estimated with the viscoelastic model.

2014; Saria *et al.* 2014) jointly indicates that Nubia-Antarctic plate motion has been steady since at least 5.2 Ma and that outward displacement between Nubia and Antarctica is 5 km. The DMS15 and geodetic estimates of Nubia-Antarctic plate motion are both 10–15 per cent slower than given by the 3.16-Myr-average MORVEL angular velocity, primarily because the latter was calibrated for only 2 km of assumed outward displacement (DeMets *et al.* 2010). Seafloor spreading rates determined from the numerous DMS15 identifications of magnetic reversals back to 5.24 Ma reduce non-closure around the Bouvet triple junction relative to that reported in the MORVEL study, indicating that the DMS15 estimate of Nubia-Antarctic motion is consistent with other plate kinematic observations from the Nubia-Antarctic-Sur three-plate circuit.

Lwandle-Antarctic plate velocities estimated from the DMS15 reconstructions of the central third of the Southwest Indian Ridge also agree better with a geodetic estimate of Lwandle-Antarctic motion than do velocities estimated with MORVEL and indicate that motion between the two plates has been steady since 5.2 Myr.

Somalia-Antarctic plate motion estimated with DMS15 angular velocities for the past 5.2 Ma is more similar to geodetic estimates than are velocities determined with MORVEL (Fig. 2), which are too fast by ∼5–10 per cent. A 0.5–1.5 mm yr^{-1} difference between Somalia-Antarctic opening rates estimated with the GPS and DMS15 angular velocities may result from a combination of sparse GPS coverage of the Somalia plate and/or systematic biases in GPS velocities due to glacial isostatic adjustment in Antarctica and/or post-seismic deformation triggered by the 2004 Sumatra or other large regional earthquakes. Though less likely, some of the difference may also be explained by a modest error in the 2 km calibration that was used by DMS15 to correct for outward displacement for this plate pair or uncertainties in the location where the western boundary of the Somalia plate intersects the Southwest Indian Ridge. The DMS15 estimate of Somalia-Antarctic plate motion is consistent with closure of the Capricorn-Somalia-Antarctic plate circuit and, given its better agreement with geodetic estimates, most likely describes Somalia-Antarctic plate motion more accurately than does MORVEL.

ACKNOWLEDGEMENTS

We thank Matt King and an anonymous reviewer for comments that lead to substantial improvements to this manuscript. This work was supported by U.S. National Science Foundation grants OCE-0926274 and OCE-1433323 (DeMets) and EAR-0538119 (Calais). Figures were drafted using Generic Mapping Tools software (Wessel & Smith 1991). We are grateful for open access to continuous GPS data from a variety of sources, including the Plate Boundary Observatory operated by UNAVCO and supported by National Science Foundation grants EAR-0350028 and EAR-0732947, the Global GNSS Network operated by UNAVCO for NASA Jet Propulsion Laboratory under NSF cooperative agreement no. EAR-0735156, and SONEL (www.sonel.org).

REFERENCES

Altamimi, Z., Collilieux, X. & Metivier, L., 2011. ITRF2008: an improved solution of the international terrestrial reference frame, *J. Geod.,* **8,** 457–473.

Argus, D.F., 2007. Defining the translational velocity of the reference frame of Earth, *Geophys. J. Int.,* **169,** 830–838.

Argus, D.F., 2012. Uncertainty in the velocity between the mass center and surface of Earth, *J. geophys. Res.,* **117,** B10405, doi:10.1029/2012JB009196.

Argus, D.F., Blewitt, G., Peltier, W.R. & Kreemer, C., 2011. Rise of the Ellsworth mountains and parts of the East Antarctic coast, *Geophys. Res. Lett.,* **38,** L16303, doi:10.1029/2011GL048025.

Atwater, T. & Mudie, J.D., 1973. Detailed near-bottom geophysical study of the Gorda Rise, *J. geophys. Res.,* **78,** 8665–8686.

Banerjee, P., Pollitz, F., Nagarajan, B. & Burgmann, R., 2007. Coseismic slip distributions of the 26 December 2004 Sumatra-Andaman and 28 March 2005 Nias earthquakes from GPS static offsets, *Bull. seism. Soc. Am.,* **97,** S86–S102.

Chlieh, M. *et al.*, 2007. Coseismic slip and afterslip of the great M_w 9.15 Sumatra-Andaman earthquake of 2004, *Bull. seism. Soc. Am.,* **97,** S152–S173.

DeMets, C. & Wilson, D.S., 2008. Toward a minimum change model for recent plate motions: calibrating seafloor spreading rates for outward displacement, *Geophys. J. Int.,* **174,** 825–841.

DeMets, C. & Merkouriev, S., 2016. High-resolution reconstructions of Pacific-North America plate motion: 20 Ma to present, *Geophys. J. Int.,* **207,** 741–773.

DeMets, C., Gordon, R.G. & Argus, D.F., 2010. Geologically current plate motions, *Geophys. J. Int.,* **181,** 1–80.

DeMets, C., Merkouriev, S. & Sauter, D., 2015. High-resolution estimates of Southwest Indian Ridge plate motions, 20 Ma to present, *Geophys. J. Int.,* **203,** 1495–1527.

Dick, H.J.B. *et al.*, 1991. Tectonic evolution of the Atlantis II Fracture Zone, in *Proceedings of the Ocean Drilling Program, Scientific Results,* eds Herzen, R.P. *et al.*, Vol. 118, pp. 359–398, College Station, TX.

Freed, A.M., Hirth, G. & Behn, M.D., 2012. Using short-term post-seismic displacements to infer the ambient deformation conditions of the upper mantle, *J. geophys. Res.,* **117,** B01409, doi:10.1029/2011JB008562.

Gordon, R.G., Stein, S., DeMets, C. & Argus, D.F., 1987. Statistical tests for closure of plate motion circuits, *Geophys. Res. Lett.,* **14,** 587–590.

Horner-Johnson, B.C., Gordon, R.G. & Argus, D.F., 2007. Plate kinematic evidence for the existence of a distinct plate between the Nubian and Somalian plates along the Southwest Indian Ridge, *J. geophys. Res.,* **112,** B05418, doi:10292006JB004519.

Iaffaldano, G., Hawkins, R., Bodin, T. & Sambridge, M., 2014. REDBACK: open-source software for efficient noise-reduction in plate kinematic reconstructions, *Geochem. Geophys. Geosys.,* **15,** 1663–1670.

James, T.S., Gowan, E.J., Wada, I. & Wang, K., 2009. Viscosity of the asthenosphere from glacial isostatic adjustment and subduction dynamics at the northern Cascadia subduction zone, British Columbia, Canada, *J. geophys. Res.,* **114,** B04405, doi:10.1029/2008JB006077.

King, M.A. & Santamaria-Gomez, A., 2016. Ongoing deformation of Antarctica following recent great earthquakes, *Geophys. Res. Lett.,* **43,** 1918–1927.

King, M.A., Whitehouse, P.L. & VanderWal, W., 2016. Incomplete separability of Antarctic plate rotation from glacial isostatic adjustment deformation within geodetic observations, *Geophys. J. Int.,* **204,** 324–330.

Kreemer, C., Blewitt, G. & Klein, E.C., 2014. A geodetic plate motion and Global Strain Rate Model, *Geochem. Geophys. Geosys.,* **15,** 3849–3889.

Kumar, R.V. & Gordon, R.G., 2009. Horizontal thermal contraction of oceanic lithosphere: the ultimate limit to the rigid plate approximation, *J. geophys. Res.,* **114,** B01403, doi:10.1029/2007JB005473.

Macdonald, K.C., 1977. Near bottom magnetic anomalies, asymmetric spreading, oblique spreading and tectonics of the Mid-Atlantic Ridge near Lat 37°N, *Bull. geol. Soc. Am.,* **88,** 541–555.

Merkouriev, S. & DeMets, C., 2008. A high-resolution model for Eurasia-North America plate kinematics since 20 Ma, *Geophys. J. Int.,* **173,** 1064–1083.

Merkouriev, S. & DeMets, C., 2014. High-resolution Quaternary and Neogene reconstructions of Eurasia-North America plate motion, *Geophys. J. Int.,* **198,** 366–384.

Molnar, P. & Stock, J.M., 2009. Slowing of India's convergence with Eurasia since 20 Ma and its implications for Tibetan mantle dynamics, *Tectonics,* **28,** TC3001, doi:10.1029/2008TC002271.

Pollitz, F.F., 1997. Gravitational viscoelastic postseismic relaxation on a layered spherical Earth, *J. geophys. Res.,* **102,** 17 921–17 941.

Pollitz, F.F., Burgmann, R. & Romanowicz, B., 1998. Viscosity of oceanic asthenosphere inferred from remote triggering of earthquakes, *Science,* **280,** 1245–1249.

Pollitz, F.F., Burgmann, R. & Banerjee, P., 2006. Post-seismic relaxation following the great 2004 Sumatra-Andaman earthquake on a compressible self-gravitating Earth, *Geophys. J. Int.,* **167,** 397–420.

Pollitz, F., Banerjee, P., Grijalva, K., Nagarajan, B. & Burgmann, R., 2008. Effect of 3-D viscoelastic structure on post-seismic relaxation from the 2004 $M = 9.2$ Sumatra earthquake, *Geophys. J. Int.,* **173,** 189–204.

Royer, J.-Y., Gordon, R.G. & Horner-Johnson, B.C., 2006. Motion of Nubia relative to Antarctica since 11 Ma: implications for Nubia-Somalia, Pacific-North America, and India-Eurasia motion, *Geology,* **34,** 501–504.

Saria, E., Calais, E., Stamps, D.S., Delvaux, D. & Hartnady, C.J.H., 2014. Present-day kinematics of the East African Rift, *J. geophys. Res.,* **119,** 3584–3600.

Sempere, J-C., Macdonald, K.C. & Miller, S.P., 1987. Detailed study of the Brunhes/Matuyama reversal boundary on the East Pacific Rise at 19°30′ S: implications for crustal emplacement processes at an ultra fast spreading center, *Mar. Geophys. Res.,* **9,** 1–23.

Sempere, J.-C., Kristjansson, L., Schouten, H., Heirtzler, J.R. & Johnson, G.L., 1990. A detailed magnetic study of the Reykjanes Ridge between 63°00′ N and 63°40′ N, *Mar. Geophys. Res.,* **12,** 215–234.

Tregoning, P., Burgette, R., McClusky, S.C., Lejeune, S., Watson, C.S. & McQueen, H., 2013. A decade of horizontal deformation from great earthquakes, *J. geophys. Res.,* **118,** 2371–2381.

Wessel, P. & Smith, W.H.F., 1991. Free software helps map and display data, *EOS, Trans. Am. geophys. Un.,* **72,** 441–446.

Wilson, D.S., McCrory, P.A. & Stanley, R.G., 2005. Implications of volcanism in coastal California for the Neogene deformation history of western North America, *Tectonics,* **24,** TC3008, doi:10.1029/2003TC001621.

Wu, X., Collilieux, X., Altamimi, Z., Vermeersen, B.L.A., Gross, R.S. & Fukumori, I., 2011. Accuracy of the International Terrestrial Reference Frame origin and Earth expansion, *Geophys. Res. Lett.,* **38,** L13304, doi:10.1029/2011GL047450.

SUPPORTING INFORMATION

Additional Supporting Information may be found in the online version of this paper:

Somalia_GPS
Nubia_GPS
Antarctic_GPS (http://gji.oxfordjournals.org/lookup/suppl/doi:10.1093/gji/ggw386/-/DC1).

Please note: Oxford University Press is not responsible for the content or functionality of any supporting materials supplied by the authors. Any queries (other than missing material) should be directed to the corresponding author for the paper.